17th World Conference on Earthquake Engineering, 17WCEE
Sendai, Japan - September 13th to 18th 2020

Seismic performance upgrading for underground structures by introducing lead-filled steel tube dampers

Zhiming. He[(1)], Qingjun. Chen[(2)]

[(1)] Ph.D student, Department of Structural Engineering and Disaster Reduction, Tongji University, Shanghai/200092, chiming@tongji.edu.cn
[(2)] Professor, Department of Structural Engineering and Disaster Reduction, Tongji University, Shanghai/200092, China, chenqj@tongji.edu.cn

Abstract

Large-space underground structures such as underground subway stations, underground commercial streets and underground parking lots, are widely used urban construction measures. However, seismic investigation demonstrates that the deformation of the surrounding soil around the underground structure can be very large under strong earthquakes, which may damage the weakest position of the structure, affecting the stability of the entire structural system. Once the structure is destroyed, the repair work is difficult, time-consuming and expensive. Therefore, it is necessary to improve the seismic safety of underground structures. Because the damage of large-space underground structures is mainly caused by the insufficient seismic capacity of the central column, therefore, improving the seismic performance of the central column is the key. Generally, the feasible means includes increasing the cross-sectional dimension, the reinforcement ratio and the material strength of the structural component. However, these methods increase their own inertial force while increasing the stiffness of the components. In addition, it will also reduce the ductility of the components. Therefore, new measures should be adopted. Passive control technology is an alternative way, which the dampers can be used to separate the central column from the top slab. As a result, the vertical bearing capacity of the central column can be ensured by controlling its lateral deformation, due to part of the deformation of central column is transferred to the damper. As a new type of metallic-combined damper, Lead-filled steel tube damper (LFSTD) possesses the merits of stable working performance, good ductility and isotropic in the working plane of the vertical axis, which is a good choice applied to large-space underground structures. However, researches of LFSTDs mainly aims to the application of aboveground structures. However, due to the underground structure is constrained by the surrounding soil, the dynamic response of the structure generally does not obviously exhibit self-vibration characteristics. Therefore, there is a big difference between the aseismic design of underground structures and aboveground structures. In this research, an aseismic scheme by utilizing Lead-filled Steel Tube Damper (LFSTD) to reduce the seismic response of central columns is proposed. Firstly, the specific idea and implementation form of the proposed scheme are illustrated. Then, with the Daikai subway station as research background, three-dimensional nonlinear dynamic response of the structure with or without the LFSTD under the Hanshin earthquake are compared, considering the soil-underground structure interaction effect. The feasibility and effectiveness of the proposed scheme are verified from four aspects: force, deformation, damage and energy dissipation, respectively.

Keywords: underground structures; Lead-filled steel tube damper; soil-structure interaction; seismic response analysis

1. Introduction

Large-space underground structures such as underground subway stations, underground commercial streets and underground parking lots, are widely used urban construction measures in China. Especially in public transportation field, over 2000 subway stations have been constructed till 2015, and over 370 stations were constructed in 2016. However, seismic investigation indicates that the deformation of the surrounding soil around underground structures can be quite large under strong earthquakes, which may destruct the weakest position of the structure, affecting the stability of the entire structural system [1, 2]. Therefore, it is necessary to ensure the seismic safety of underground structures under strong ground shakings.

The failure mechanisms of large-space underground structures have demonstrated that the structural damage is mainly caused by the insufficient seismic capacity of central columns [3, 4]. Therefore, to improve the seismic capacity of large-space underground structures, upgrading the seismic performance of the central column is the key. Generally, the feasible means includes increasing the cross-sectional dimension, the reinforcement ratio and the material strength to the structural component [5, 6]. However, these methods can increase their own inertial force while increasing the stiffness. Moreover, the ductility of the component can also be reduced. Therefore, measures can balance the stiffness and ductility of the central column should be adopted. Seeing from the practices of aboveground structures, it is an effective measure to improve the seismic performance of structures by dissipating seismic energy through metallic deformation [7, 8]. Thus, metallic dampers can be used to separate the central column from the top beam in underground structures. By utilizing the deformation capacity of the damper, partial deformation of the central column will be transferred to the damper. Since the lateral deformation of the central columns is being controlled, the bearing capacity of the central column can be guaranteed.

As a new type of metallic-combined damper, Lead-filled steel tube damper (LFSTD) possesses the merits of stable working performance, good ductility and isotropic in the working plane of the vertical axis [9, 10]. In addition, axial compressive deformation has minor influence on the hysteretic performance of the LFSTD. Therefore, LFSTD is chose to improve the seismic performance of large-space underground structures. Recently, experimental studies on seismic performance of LFSTDs have been carried out. Additionally, studies about parameter optimization and design procedure have also been conducted. Zhou et al. found that partially weaken the middle of the steel tube can control the stress distribution of the LFSTD effectively, which can prevent the LFSTD being failure due to the damage of the end connection [9]. Lu et al. optimized the thickness of the transition section from same thickness to variable thickness to the LFSTD. The results demonstrated that the optimized LFSTD can effectively improve the stress distribution and the failure mode of the steel tube [10]. In addition, Lu et al. also found that the reasonable value of thickness-diameter ratio, weakening ratio and height-diameter ratio of the LFSTD can ensure that the energy dissipation is concentrated in the middle of the damper, forming a reasonable plastic distribution pattern [11]. As for application, He et al. applied the LFSTD to the replaceable shear link and gave the design suggestions for the damper [12].

However, the abovementioned research of LFSTDs mainly aims to aboveground structures. As underground structures are constrained by the surrounding soil, the dynamic response of the structure generally does not obviously exhibit self-vibration characteristics [13, 14], while aboveground structures are controlled by inertial forces. Therefore, the achievements on aseismic design of aboveground structures cannot be directly applied on underground structures. In this study, to explore the feasibility of applying the LFSTD to large-space underground structures, three-dimensional nonlinear dynamic analyses of the Daikai subway station with and without LFSTDs under the Hyogoken-Nambu earthquake are carried out, considering the soil-structure interaction effect. A simplified bilinear restoring model is utilized to simulate the hysteretic behavior of the LFSTD. Base on the aspects of force, deformation, damage and energy dissipation, the feasibility of applying the LFSTD to large-space underground structures is verified.

2. Application of LFSTDs in underground structures

2.1 Introduction of LFSTD

LFSTD is a combined displacement-type damper, which is mainly composed of steel tube, lead core, extrusion head and connecting plate, as shown in Figure 1 (a). Steel tube is the main energy dissipation component, which accounts for over 80% of the total energy dissipation of the damper. While the function of the lead core is to restrain the buckling of the steel tube. The working mechanism of the LFSTD is as follows: in a minor earthquake, both steel tube and lead core are in elastic state. The LFSTD only provides the stiffness to the structure. Then, with the earthquake intensity increases, the deformation (mainly in shear direction) of the LFSTD increases gradually. The lead core yields firstly under the subjected shear deformation extrusion. Finally, with the earthquake intensity further increases, steel tube also enters the yield state, dissipating the inputted seismic energy with the lead core. At this state, LFSTD can provide the additional damping to the structure.

The force-deformation characteristics of the metallic damper under seismic loading are often been approximated through discrete multi-linear models, such as the ideal elastoplastic model and the bilinear model. In order to facilitate the identification of parameters involved in designing typical dampers, bilinear model with kinematic hardening rule, as shown in Figure 1 (b), is adopted to describe the hysteretic behavior of the LFSTD. In the model, initial stiffness (K_1) consists of the elastic stiffness of the steel tube (K_s) and the lead core (K_l). K_s is determined as follows [15]:

$$K_s = \frac{1}{\int_{-\frac{h}{2}}^{\frac{h}{2}} \frac{\kappa}{G_S A_S} d_Z + \int_{-\frac{h}{2}}^{\frac{h}{2}} \frac{Z \cdot Z}{E_S I_S} d_Z} \tag{1}$$

Where, E_S and G_S are the elastic modulus and shear modulus of the steel respectively. A_S represents the cross-section area, and I_S represents the moment of inertial of the cross section of the steel tube. κ is the correction factor due to the inhomogeneous distribution of the shear stress along the cross section, which is determined by the sectional form. For thin-walled ring sections, the value of κ is often taken as 2. K_l is determined as follows [15]:

$$K_l = \frac{0.09\pi}{4} \frac{E_l \cdot d^4}{\left(\sqrt{d^2 + h^2}\right)^3} \tag{2}$$

Where, d and h are the diameter and height of the lead core respectively. E_l is the elastic modulus of the lead. The post-yield stiffness (K_2) is about 0.01 to 0.03 of the initial stiffness.

Similar to the stiffness of the LFSTD, the yield force of the LFSTD (F_y) consists of the yield force of the steel tube (F_{ys}) and the lead core (F_{yl}). F_{ys} is determined as follows [15]:

$$F_{ys} = m \cdot f_{ys} \cdot A_S \tag{3}$$

Where, f_{ys} is the shear strength of the steel tube, and m is the coefficient considering the influence of the thickness-diameter ratio, weakening ratio and height-diameter ratio of the LFSTD. F_{yl} is determined as follows [15]:

$$F_{yl} = \frac{0.09\pi}{4} \cdot d^4 \cdot f_{yl} \cdot cos\theta \tag{4}$$

Where, f_{yl} is the shear strength of the lead.

2.2 Overview of the proposed aseismic scheme in underground structures

The LFSTD is installed between the upper end of the central column and the top beam. The working mechanism of the proposed scheme under static and dynamic loads is presented in Figure 2. During an earthquake, the seismic loads which are normally produced through the deformation and strain of the surrounding soil accompany with the static loads subject to the underground structure, compelling the structure to produce the corresponding deformation. At the initial stage, the force and deformation which are transferred from the top beam firstly act on the LFSTD. The LFSTD will be in an elastic or inelastic state base on the degree of the deformation. In a minor earthquake, the deformation of the LFSTD is relatively small. Therefore, the LFSTD maintains in elastic state and can provide the stiffness to the structure. With the earthquake intensity increases, the deformation of the damper increases gradually and enters the elastic-plastic or plastic stage. At this time, LFSTD can dissipate partial inputted seismic energy and provide the additional damping to the structure.

Figure 3 (a) describes the relationship between LFSTD and the central column, which are in series. Two springs represent the LFSTD and the central column, respectively. Figure 3 (b) exhibits the bilinear force-displacement model of the LFSTD and the central column. F_y and K_y represents the lateral yield force and initial elastic stiffness, respectively. D_y represents the yield displacement. Since the purpose of the LFSTD is to dissipate energy generated in the structure through plastic deformation in the LFSTD, therefore, to control the central column in minor or even no damage in the proposed scheme, LFSTD is designed to enter plastic state prior to the central column. It means the horizontal yield strength of the central column (Fy,Central column) to be designed exceeding that of the LFSTD (Fy,LFSTD).

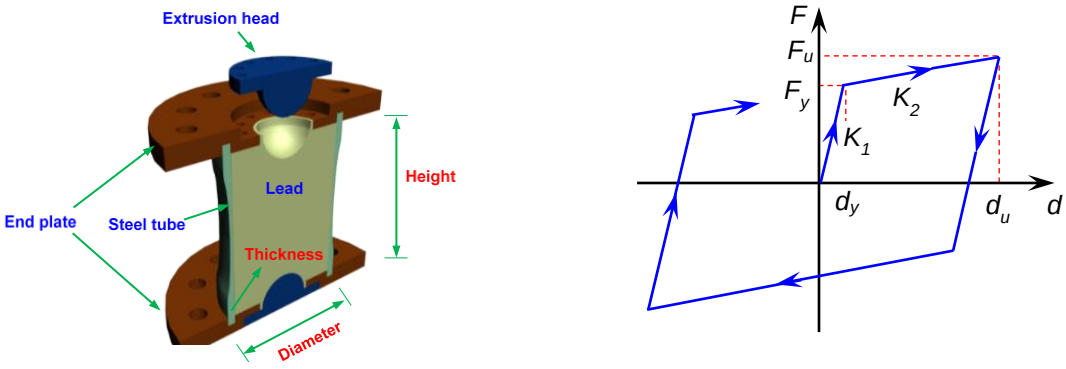

(a) *(b)*

Figure 1. (a) Configuration profile and (b) bilinear model of the LFSTD.

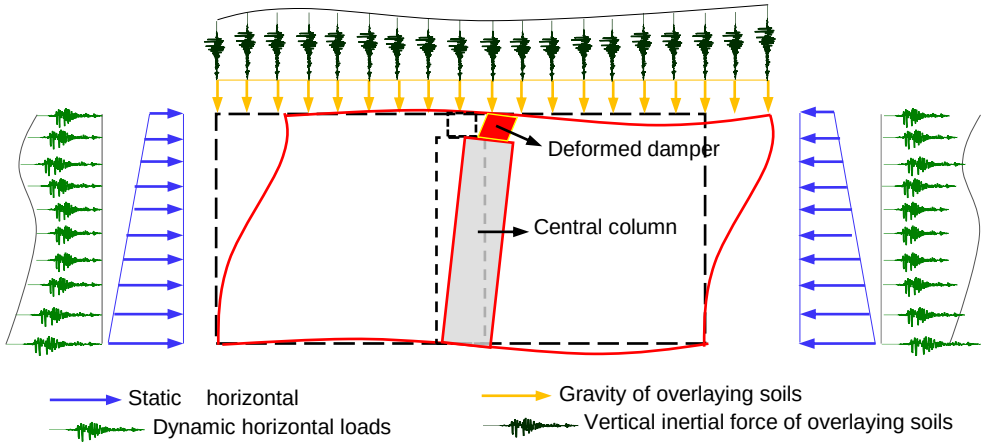

Figure 2. Working mechanism of the proposed scheme under static and dynamic loading.

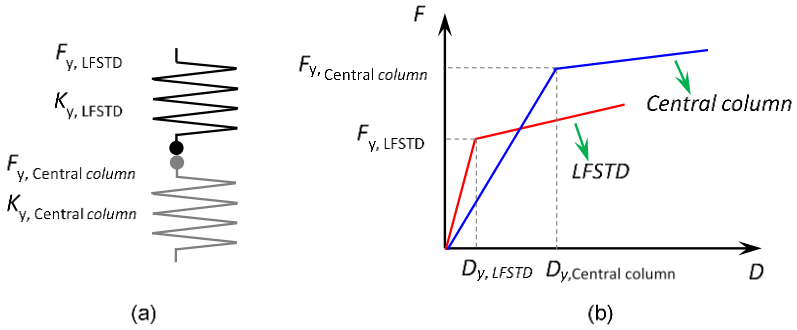

Figure 3. (a) Relationship between the LFSTD and the central column and (b) bilinear force-displacement curves of the central column and the LFSTD

3. Seismic effectiveness of applying LFSTD in underground structures

3.1 Target structure and numerical model

Daikai subway station is selected as the research background in this study. The cross-sectional dimension of the station is depicted in Figure 4.(a). As shown in the figure, the overburden, height, and width of the subway are 4.8, 7.17, and 17 m, respectively. Figure 4.(b) displays the reinforcement details of central columns. To verify the effectiveness of applying the LFSTD in large-space underground structures, a

detailed soil-underground subway station interaction analysis model is developed using the finite element code ABAQUS. In the 3D numerical model, depth of the analytical domain is 35 m, which is the thickness of the assumed soil deposit. The width of the analytical model mainly depends on two factors: the distance between the underground subway station and free-field zone, and the reflection of the lateral boundary. We select 350 m (i.e. 10 times of the assumed soil deposit thickness) as the width of the analytical model, which has been validated as sufficiently large to get rid of the influence of the boundary conditions as suggested by many design codes (e.g. [16]). The calculation domain and element mesh of the models are depicted in Figure. 6.

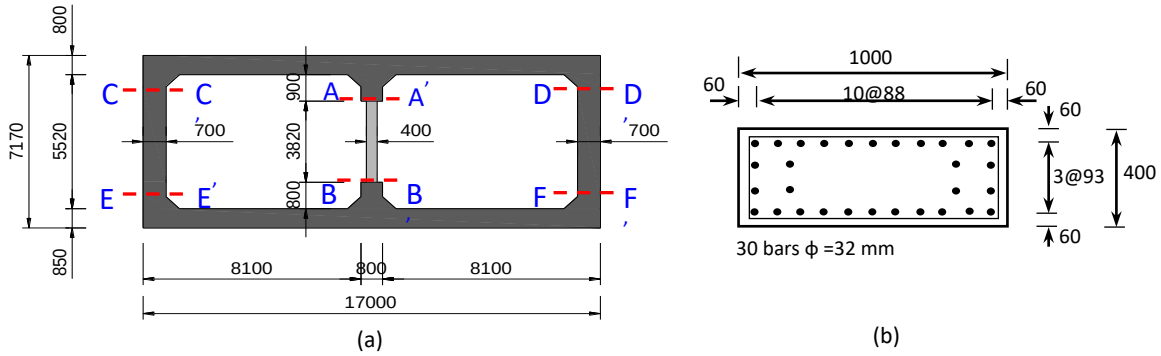

Figure 4. (a) Cross section of the Daikai subway station and (b) reinforcement details of central columns (unit: mm).

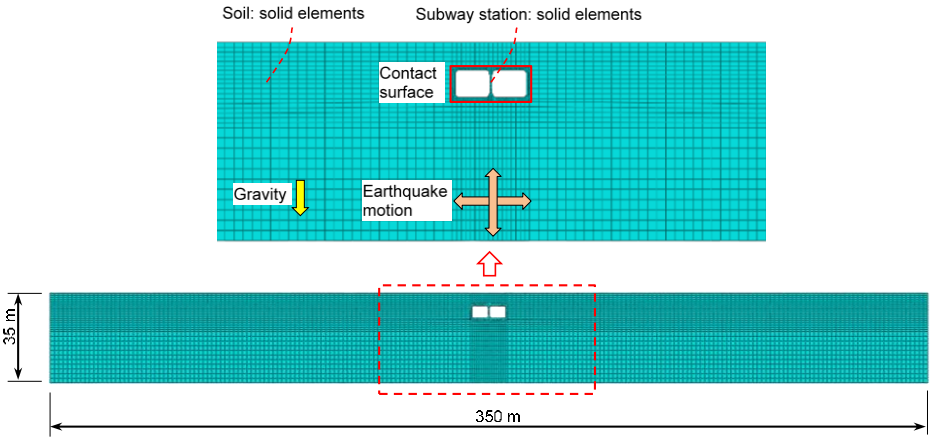

Figure 5. Finite element model.

The inelastic response characteristics of the surrounding soil is simulated through an elasto-plastic model. The corresponding mechanical properties (i.e. the shear velocity (V_s), the unit weight (γ), the poisson ratio (υ), the cohesion (c) and the friction angle (φ)) of different soils are listed in Table 1. The plasticity of soil is characterized by the cohesion and the friction angle. As for the station, the plastic-damage model [17] is adopted. The model assumes the uniaxial tensile and compressive behavior of concrete are characterized through damage plasticity. During the analysis, the crucial parameters of the plastic-damage model (presented in Table 2) is used to describe the material properties and deformation behavior of the concrete. The idealized elastoplastic model is selected for the steel bars, with the density of 7800 kg/m^3, Poisson's ratio of 0.1, Young's modulus of 200 GPa and yield stress of 240 MPa.

Penalty Function Method is used to model the contact property between the soil and the station. In the normal direction of the interface, we define a hard contact. The normal contact compressive stress can mutually transfer via the contact constraint. The element nodes on the interface satisfy Hooke's Law and the Harmonized Condition of Displacement. In the tangential direction of the interface, tangential contact shear

stress is also transferred, and we assume that tangential mechanics behavior of the interface follows the Coulomb friction law with a friction coefficient, μ, of 0.4. This contact relationship was commonly used by different researchers [3, 20, 21].

Table 1. Soil physical properties.

Soil layer	Depth (m)	Soil type	Unit weight (kg·m^{-3})	Shear wave velocity (m·s^{-1})	Poisson ratio	Cohesion (kPa)	Friction angle (°)
1	1.6	Backfill	1950	100	0.333	0	20
2	3.2	Clay	2050	140	0.488	20	0
3	4.8	Sand	2000	220	0.488	0	25
4	6.8	Sand	2000	220	0.493	0	25
5	12.0	Clay	2000	190	0.494	50	0
6	13.0	Sand	2100	240	0.494	0	30
7	17.0	Sand	2050	240	0.490	0	30
8	35.0	Gravel	2200	300	0.487	50	35

Table 2. Material parameters of concrete [18].

Parameters	Value	Parameters	Value
Density	2500 kg/m^3	Limited compressive yield stress	26.8 MPa
Dilation angle	35°	Initial tensile yield stress	2.4 MPa
Elastic modulus	30 GPa	Tensile stiffness recovery parameter	0.0
Poisson's ratio	0.2	Compressive stiffness recovery parameter	1.0
Initial compressive yield stress	18.8 MPa	Damage variable	(Refer to

The soil and the station are meshed with 8-nodes reduced integration linear solid element (C3D8R), while the reinforcement is modeled with three-node linear beam elements (B31). In dynamic analysis, the element mesh for soil is based on Liao's study [22], which can ensure the efficient reproduction of all the waveforms of whole frequency range under study, the maximum height of element h_{max} in soil is determined as

$$h_{max} = \frac{\left(\frac{1}{75} - \frac{1}{160}\right) V_s}{f_{max}} \tag{5}$$

where V_s is the shear and compression motion velocity, which can be determined through $G_0=\rho Vs^2$, ρ is the density of soil, and f_{max} is the maximum vibration frequency of the inputted motion. Therefore, the maximum heights of the element are 1m to 3m from the surface to bottom. A finer discretization is adopted near the station structure.

During the analyses, we simplified the LFSTD in simulation through one horizontal spring and one vertical spring which as presented in Figure 6. For the horizontal spring, the force-displacement relationship which is in accordance with that of a real LFSTD device, is used to simulate the displacement and the shear force of the LFSTD under horizontal load through the bilinear model. The horizontal initial stiffness of the LFSTD is calculated through Eq.(1) and Eq.(2). The horizontal post-yield stiffness is taken as 0.02 of the horizontal initial stiffness. The vertical spring is used to transfer the axial load from the top beam to the central column. In the preliminary discussion on the feasibility of the proposed scheme, a test specimen with the dimension of a height of 300 mm, a thickness of 15 mm of the steel tube, and a diameter of 150 mm of the lead core is adopted. Correspondingly, the yield force and yield deformation of the LFSTD are 186.4 kN and 1 mm, respectively.

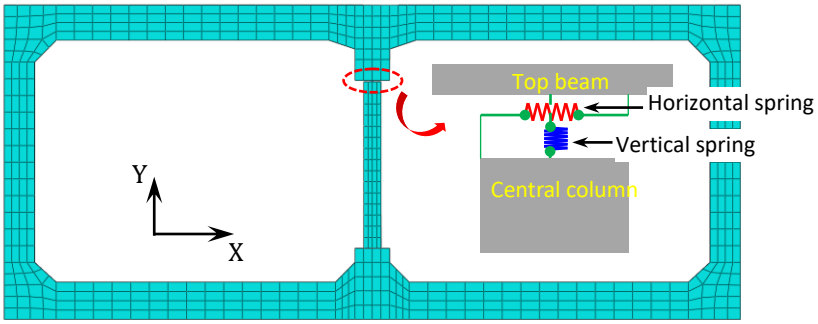

Figure 6. FEM model of the beam-LFSTD-column system.

The analyses are conducted in three steps. First step is the static stress equilibrium analysis, which is to obtain the horizontal reaction forces (RF) at the nodes of the lateral boundaries. During this step, the nodes in the horizontal direction of the lateral boundaries of the analysis model are constrained, and the base is fixed in the horizontal and vertical directions. The subsequent step is to substitute the horizontal displacement restraints with RF, and the vertical displacement at the nodes of the lateral boundaries are fixed. The final step is a dynamic analyses step, the horizontal and vertical seismic acceleration is applied uniformly along the base of the model, and the bottom are free in the horizontal and vertical direction.

The horizontal and vertical component of the records are presented in Figure 7. The frequency content of the ground motion is mainly below 10 Hz and the dominate frequency ranges from 1.5 to 2.5 Hz based on the results of Fourier Transform. We can find that the peak value of both horizontal and vertical component is at a very high level, which is 0.83 g and 0.34 g, respectively. However, the amplitude of both components is less than 10% of the peak value after 20 s. To reduce the calculation cost, a total calculation duration of 25 s is applied during the analysis.

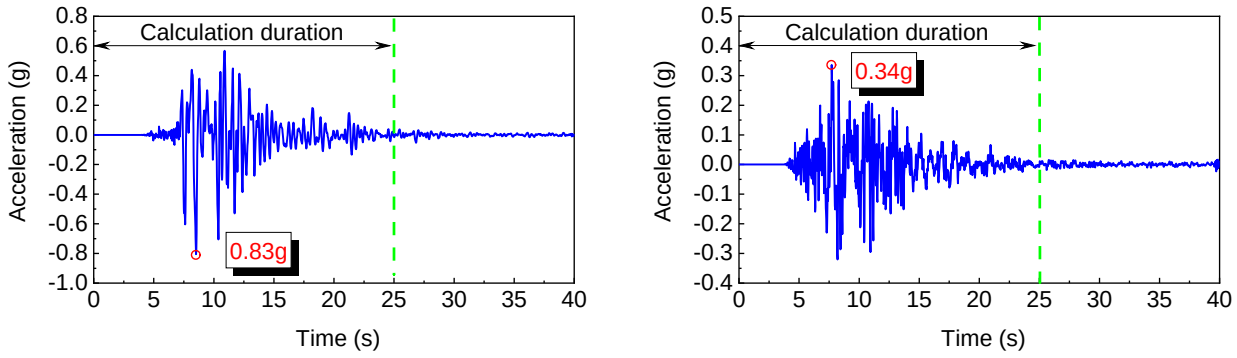

(a) (b)

Figure 7. Earthquake recordings at the Kobe meteorological observatory: (a) horizontal component and (b) vertical component

3.2 Results analysis

To investigate the seismic reduction effect before and after installing the LFSTD in the structure, section A-A', B-B', C-C', D-D', E-E' and F-F', which depicted in Figure 4 are selected as the observation section. To verify the efficiency of the proposed scheme, four aspects are selected as follows: deformation and force response of the central column, damage response of the whole structure, and behavior of the LFSTD. The results are given as follows:

3.2.1 Deformation response

The lateral and axial deformation time-history curves of the central column are shown in Figure 8. After the LFSTD is installed in the underground structure, the peak lateral deformation of the central column is

reduced from 32.2 mm to 18.2 mm, bringing a reduction of 43.8%. As for the axial deformation, the peak value is reduced from 2.96 mm to 1.58 mm, with a 46.6% reduction. The reason for the significant reduction of the lateral and axial deformation is that, for the original structure, the deformation is directly transmitted to the central column through the top beam and the bottom beam, while after installing the LFSTD in the central column, the top beam transmits the deformation to the LFSTD firstly, and then the LFSTD transmits the deformation to the central column. Therefore, the deformation which originally only undertaken by the central column is converted into common undertaken by the LFSTD and the central column. Because the yield displacement of the LFSTD is only 1 mm, the LFSTD can rapidly enter the elastic-plastic stage under the seismic loading and produce corresponding deformation. Therefore, the deformation of the central column is reduced, achieving the result of protecting the central column.

3.2.2. Force response

Figure 9 compares the axial force and shear force of the central column between the initial structure and the structure with the LFSTD. For the axial force, the change between these two situations is minor, which the latter is only 2.1% less than the former. The shear capacity under different axial loads have been given by Parra-Montesinos et al through numerical analyses. The corresponding central column shear capacity is 651 kN under the calculated axial force (4561 kN) of the initial structure, which is lower than the shear demand (697 kN) during the earthquake. It means the central column will be damaged during the earthquake, which is consistent with the seismic investigations. However, after the LFSTD being installed in the structure, the shear force of the central column is 316 kN, which is obviously less than the shear capacity, and brings a 54.7% reduction compared to the initial structure. That means the column will not be destroyed after upgrading the structural seismic performance by the LFSTD.

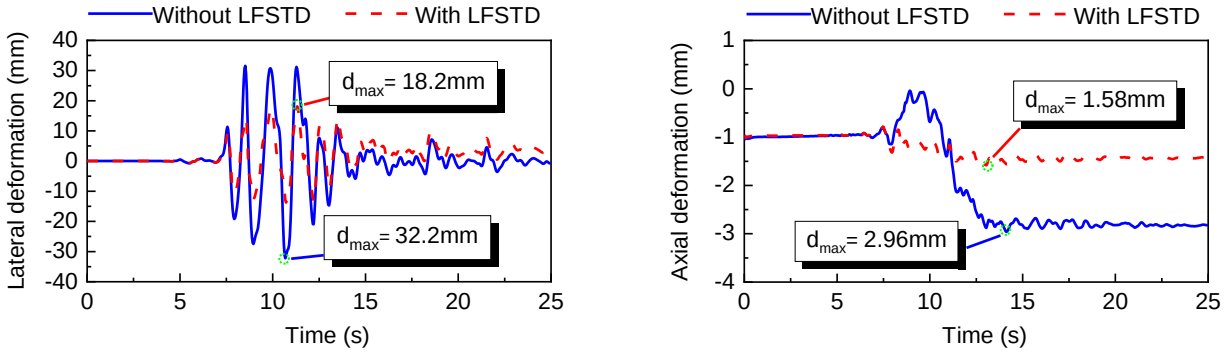

(a) *(b)*

Figure 8. Time-history curves of deformation of the central column: (a) lateral deformation and (b) axial deformation.

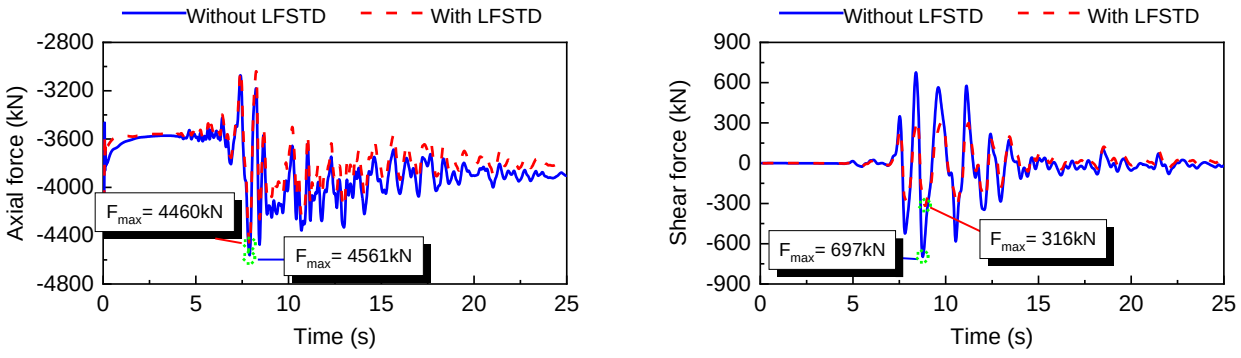

(a) *(b)*

Figure 9. Time-history curves of force of the central column: (a) axial force and (b) shear force.

3.2.3 Damage response

Time-history curves of the tensile damage (d_t) and compressive damage (d_c) on these positions are shown in Figure 15 and Figure 16. Among the damage of these positions, the change at the top of the central column is the most obvious. For the original structure, the maximum value of the d_t and d_c at the top of the central column are 0.96 and 0.79. As the damage index equal to 1 means the completely damaged state, therefore, the damage at the top of the central column of the original structure is severe. After installing the LFSTD in the central column, the maximum tensile and compressive damage drops to 0.53 and 0.12, brings about 44.8% and 84.8% reduction, respectively. Therefore, the damage of the central column can be effectively mitigated through applying the LFSTD in the central column. For the position at the bottom of the central column, although the damage is not change as obvious as the top of the central column, but the damage is also relieved after installing the LFSTD in the central column. For the mid-span of the left and right top slabs, the damage with LFSTD develops faster than the original structure under the gravity. However, the maximum value of the damage is the same in the final state. In addition, the damage development trends of the lateral wall and the bottom slab of the structure are almost synchronous before and after installing the LFSTD in the structure.

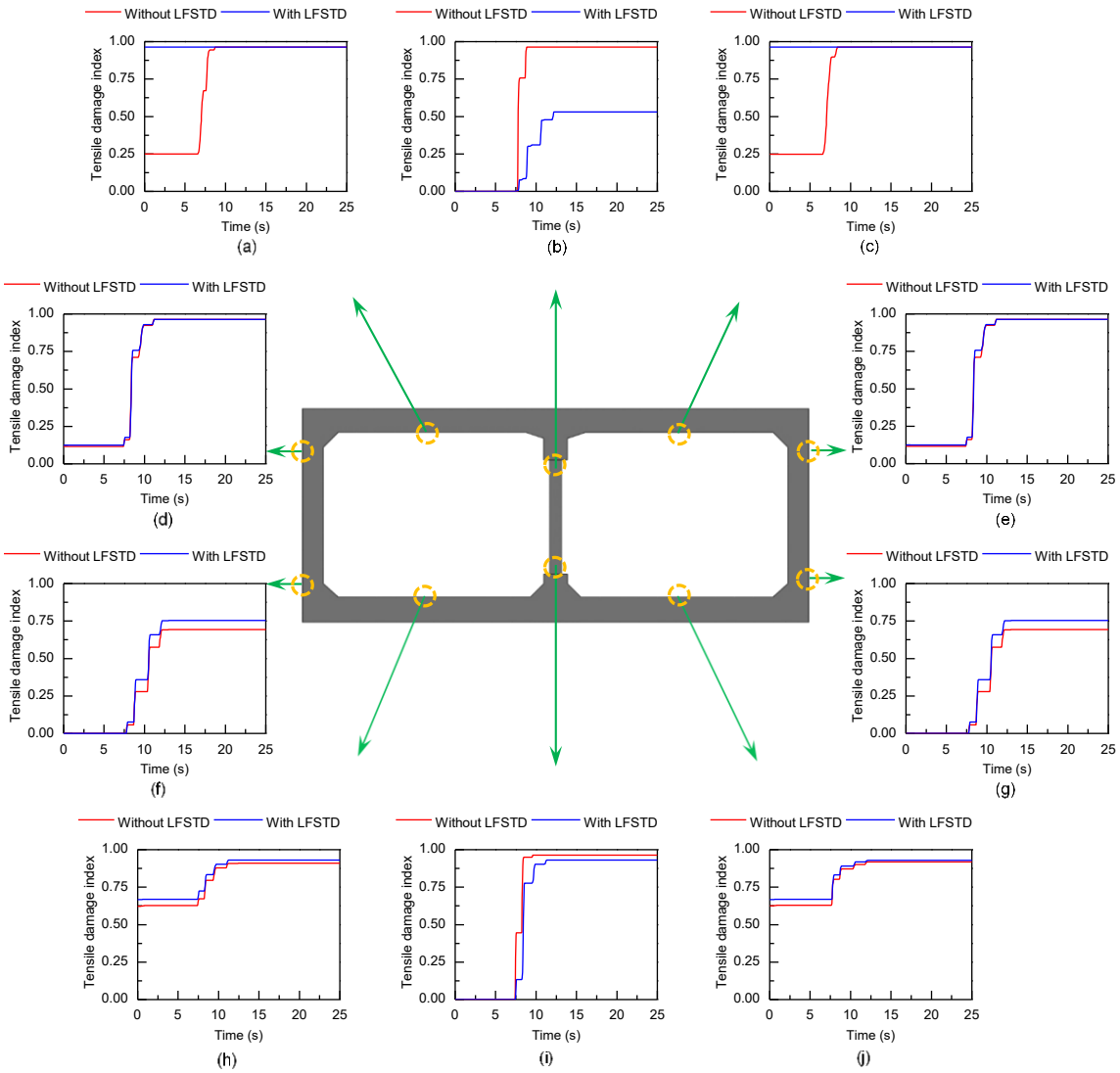

Figure 10. Time-history curves of the tensile damage

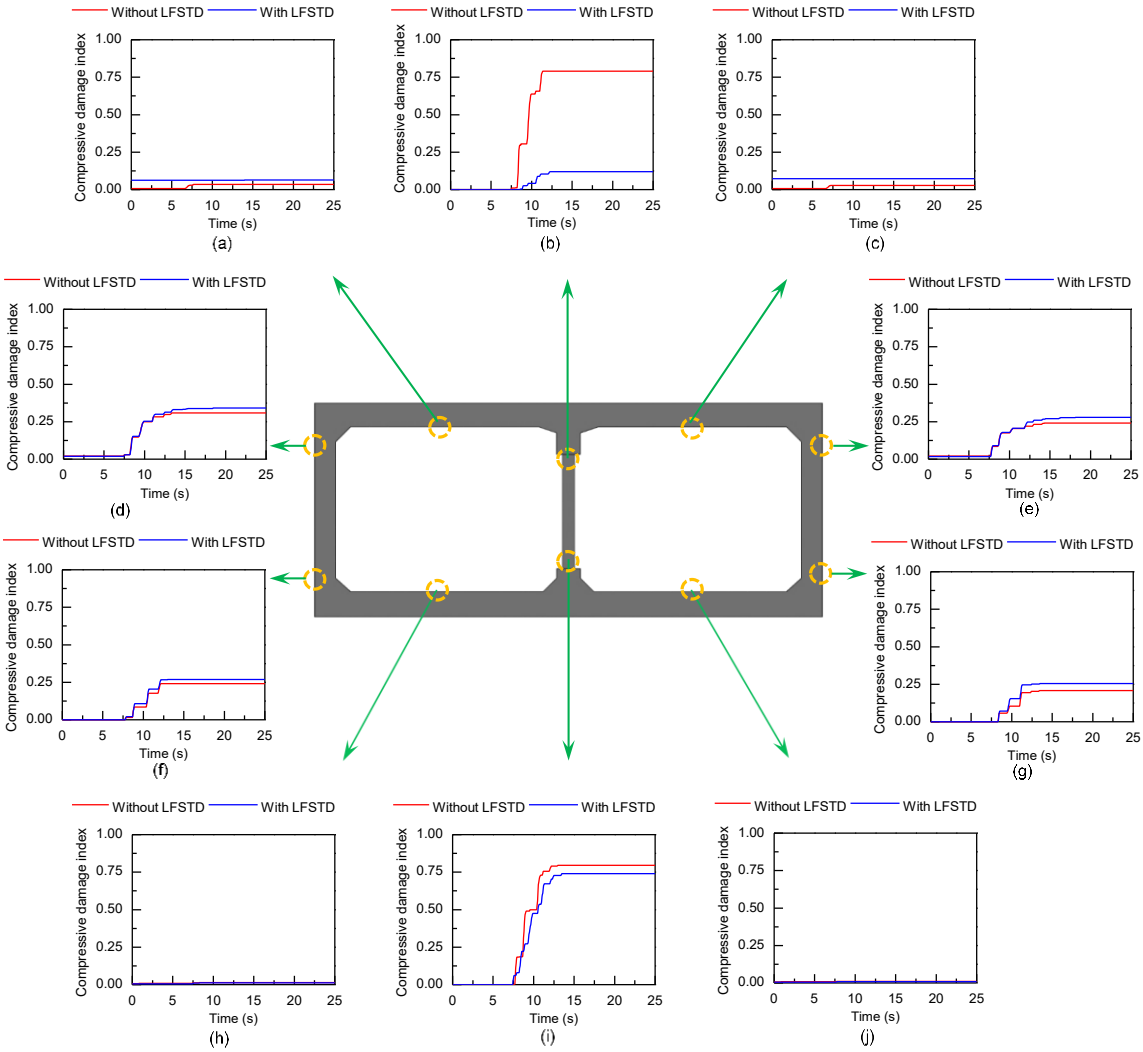

Figure 11. Time-history curves of the compressive damage

3.2.4 Energy dissipation of the LFSTD

The hysteretic curve of the LFSTD is shown in Figure 12 (a), which is stable and plumpness. The maximum shear deformation of the damper in positive and negative directions is 19.2 mm and -19.7 mm, which is less than 20 mm within the shear deformation limit. The energy dissipation development trend of the LFSTD is shown in Figure 12 (b). With the gradually increasing external inputted energy, the energy dissipated by the LFSTD gradually increases. Especially in the period between the 7.5 s to 12.4 s, the increasing trend is obvious, which means the LFSTD is more effective during intensive vibration. After 12.4 s, we can find the energy dissipation reach the maximum value of 34.4 kJ.

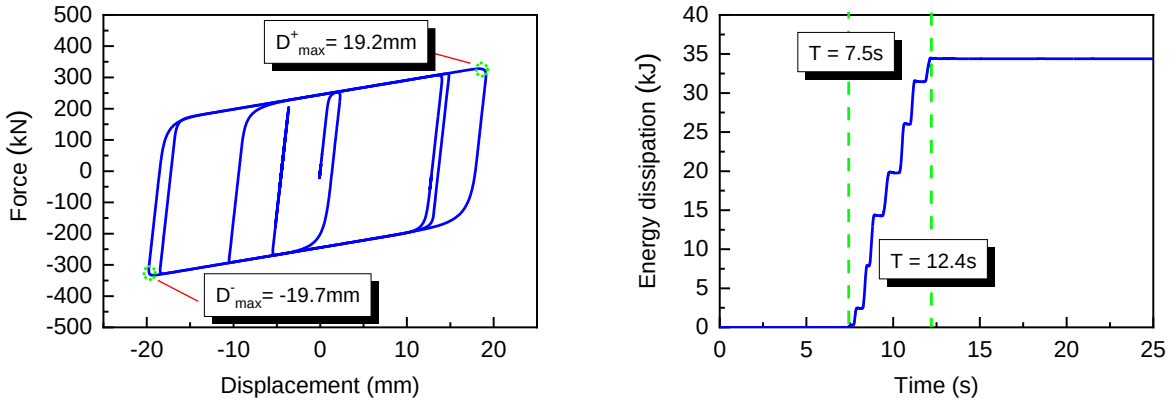

(a) *(b)*

Figure 12. (a) Hysteretic curve and (b) energy dissipation of the LFSTD.

5. Conclusion

An aseismic scheme using the LFSTD to improve the seismic performance of large-space underground structures is proposed. Taking the Dakai subway station as the research background, the feasibility of the proposed scheme is verified through the comparison of the three-dimensional nonlinear dynamic analysis of the structure with and without the LFSTD, considering the soil-structure interaction effect. The conclusions are as follows:

The application of the LFSTD to large-space underground structures can effectively reduce the force, deformation and damage of the central column under the seismic loading. The deformation and damage distribution of other structural components changes slightly after adding the LFSTD in the central column. Hence in design, it is convenient focus merely on the central column without caring the other structural components. LFSTD can dissipate the seismic energy effectively, especially during intensive vibration. Meanwhile, the maximum shear deformation of the LFSTD is less than 20 mm, which maintain the normal function.

Acknowledgments

This research is supported by the National Natural Science Foundation of China (Grant no. 51778489. All support is gratefully acknowledged.

Copyrights

Reference

1. S. Sharma and W.R. Judd, “Underground opening damage from earthquakes,” Engineering Geology, vol. 30, pp. 263-276, 1991.
2. N. Yoshida and S. Nakamura, “Damage to Daikai subway station during the 1995 Hyogoken-Nunbu earthquake and its investigation,” In: Proceedings of 11th world conference on earthquake engineering, Acapulco, Mexico, pp. 283-300, 1996.
3. H. Huo, A. Bobet and G. Fernández et al., “Load transfer mechanisms between underground structure and surrounding ground: evaluation of the failure of the Daikai station,” Journal of Geotechnical and

Geoenvironmental Engineering, vol. 131, no. 12, pp. 1522-1533, 2005.
4. G. J. Parramontesinos, “Evaluation of soil-structure interaction and structural collapse in Daikai subway station during Kobe earthquake,” Aci Structural Journal, vol. 103, no. 1, pp. 113-122, 2006.
5. G. Thermou and A.S. Elnashai, “Seismic retrofit schemes for RC structures and local-global consequences,” Progress in Structural Engineering and Materials, vol. 8, no. 1, pp. 1-15, 2006.
6. C.Z. Yue and Y.L. Zheng, “Shaking table test study on seismic behavior of underground structure with intermediate columns enhanced by concrete-filled steel tube (CFT),” Soil Dynamics and Earthquake Engineering, vol. 127, 2019.
7. T. Kobori, Y. Miura and E. Fukuzawa et al., “Development and application of hysteresis steel dampers,” In: Proceedings of 11th world conference on earthquake engineering, Acapulco, Mexico, 1996.
8. Castaldo, P., “Integrated seismic design of structure and control systems,” Springer, 2014.
9. Y. Zhou, D.H. Lu and M. Zhang et al., “Experimental investigation on hysteretic performance of lead-filled steel tube damper,” Journal of Building Structures, vol. 38, no. 9, pp. 102-109, 2017. (in Chinese)
10. D.H. Lu, Y. Zhou and X.S. Deng et al., “Optimization of configuration and finite element modeling for lead-filled steel tube dampers,” Engineering Mechanics, vol. 34, no. 3, pp. 76-83, 2017. (in Chinese)
11. D.H. Lu, Y. Zhou and X.S. Deng et al., Study of energy dissipation mechanism of lead-filled steel tube dampers, China Civil Engineering Journal, vol. 49, no. 12, pp. 49-55, 2016. (in Chinese)
12. Z.M. He, Y. Zhou and D.H. Lu et al., “Structure analysis of replaceable shear link eccentrically brace with lead-filled steel tube damper,” Earthquake Resistant Engineering and Retrofitting, vol. 38, no. 1, pp. 79-88, 2016. (in Chinese)
13. Y.M. Hashash, J.J. Hook and B. Schmidt et al., "Seismic design and analysis of underground structures," Tunnelling and Underground Space Technology, vol. 16, no. 4, pp. 247-293, 2001.
14. K. Pitilakis and G. Tsinidis, “Performance and seismic design of underground structures,” Earthquake Geotechnical Engineering Design, Springer, Cham, pp. 279-340, 2014.
15. D.H. Lu, “Study on property and application of lead-filled steel tube damper,” Doctoral dissertation, Guangzhou University, 2018.
16. C. Standard, “Code for seismic design of urban rail transit structures,” China Planning Press, Beijing, 2014.
17. J. Lee and G. L. Fenves, “Plastic-damage model for cyclic loading of concrete structures,” Journal of Engineering Mechanics, vol. 124, no. 8, pp. 892-900, 1998.
18. C. Ma, D. C. Lu and X. L. Du et al., “Effect of buried depth on seismic response of rectangular underground structures considering the influence of ground loss,” Soil Dynamics and Earthquake Engineering, Vol. 106, pp. 278-297, 2018.
19. C. Standard, “Code for design of concrete structures” China Architecture and Building Press, Beijing, 2011.
20. Z.M. He and Q.J. Chen, "Vertical seismic effect on the seismic fragility of large-space underground structures," Advances in Civil Engineering, 2019.
21. H. Liu and E. Song, "Seismic response of large underground structures in liquefiable soils subjected to horizontal and vertical earthquake excitations," Computers and Geotechnics, vol. 32, no. 4, pp. 223-244, 2005.
22. Z. Liao, "Theories of wave motion for engineering," Science Press of China, 2002.

